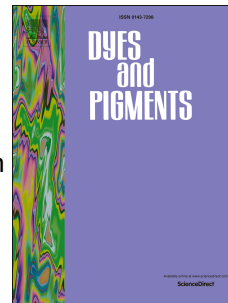


Accepted Manuscript

G-quadruplex DNA fluorescence sensing by a bis-amine-substituted styrylquinolinium dye

Ming-Qi Wang, Yuan Wu, Zi-Yu Wang, Qiu-Yun Chen, Fu-Yan Xiao, Yu-Chi Jiang, Amy Sang



PII: S0143-7208(17)30573-9

DOI: [10.1016/j.dyepig.2017.05.045](https://doi.org/10.1016/j.dyepig.2017.05.045)

Reference: DYPI 6007

To appear in: *Dyes and Pigments*

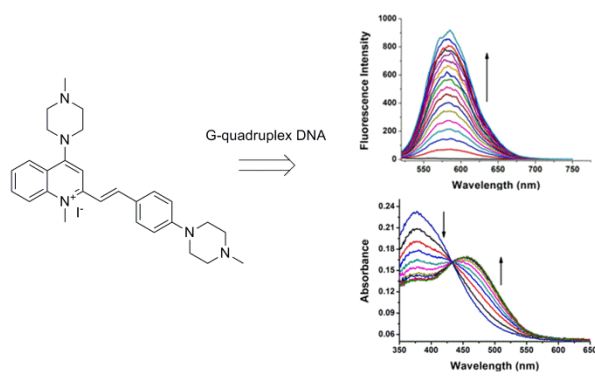
Received Date: 21 March 2017

Revised Date: 13 May 2017

Accepted Date: 23 May 2017

Please cite this article as: Wang M-Q, Wu Y, Wang Z-Y, Chen Q-Y, Xiao F-Y, Jiang Y-C, Sang A, G-quadruplex DNA fluorescence sensing by a bis-amine-substituted styrylquinolinium dye, *Dyes and Pigments* (2017), doi: 10.1016/j.dyepig.2017.05.045.

This is a PDF file of an unedited manuscript that has been accepted for publication. As a service to our customers we are providing this early version of the manuscript. The manuscript will undergo copyediting, typesetting, and review of the resulting proof before it is published in its final form. Please note that during the production process errors may be discovered which could affect the content, and all legal disclaimers that apply to the journal pertain.



G-quadruplex DNA fluorescence sensing by a bis-amine-substituted styrylquinolinium dye

Ming-Qi Wang^{a*}, Yuan Wu^a, Zi-Yu Wang^a, Qiu-Yun Chen^{b,**}, Fu-Yan Xiao^a, Yu-Chi, Jiang^a, Amy Sang^a

^a*School of Pharmacy, Jiangsu University, Zhenjiang, 212013, P. R. China*

^b*School of Chemistry and Chemical Engineering, Jiangsu University, Zhenjiang, 212013, P. R. China*

Abstract: Searching for specific G-quadruplex DNA probes is important for study of the function of G-rich gene sequence, as well as design of novel effective anticancer drugs. In this paper, a novel bis-amine-substituted styrylquinolinium dye (**BSAQ**) was designed and synthesized to enhance the performance for the application as a G-quadruplex DNA probe. The studies on **BSAQ** with different DNA forms showed that it could be used as a colorimetric and red-emitting fluorescent probe for G-quadruplex DNA. The limits of detection of **BSAQ** with various G-quadruplex DNAs were found to below 1 nM. CD spectroscopy analysis revealed that **BSAQ** did not induce the G-rich sequence folding into G-quadruplex structure. These results of this study gave some crucial factors on developing of effective probes for G-quadruplex DNA applications.

Key words: G-quadruplex DNA; probe; Bis-amine-substituted; Styrylquinolinium dye

1. Introduction

DNAs play essential roles in the storage and transfer of genetic information, which is essential for the living organisms [1]. Guanine-rich DNA sequences can form non-canonical structures known as G-quadruplexes have attracted intense scrutiny [2-4]. The basic unit of a G-quadruplex structure is the guanine tetrad that is derived from the association of four guanines into a cyclic Hoogsteen hydrogen bonding planar arrangement. Stacking of several G-tetrads leads to form a G-quadruplex motif, which can be stabilized by chelation of monovalent cations [5,6]. Computational analyses of the human DNA has revealed an abundance of putative G-quadruplex-forming sequences in the human genome. For example, G-quadruplex-forming sequences are found at the ends of the telomeres, ribosomal DNA, as well as in the important regions of oncogene promoters [7-9]. Accumulating evidence has linked G-quadruplex structures to a number of biological processes in vivo, including DNA replication, transcription, and genomic maintenance [10-13]. However, the precise function and mechanism of G-quadruplex formation in mammalian cells remains poorly defined. The research of G-quadruplex is still at an early stage. Therefore, the development of rapid and simple approaches for detection of G-quadruplex DNA structures has attracted significant attention in recent years.

Notably, visualizing G-quadruplex DNA using small-molecule probes is an extremely active area and significant progress has been made towards the development of colorimetric or fluorescent probes [14-26]. Such as the widely studied dyes based on cyanine, thiazole, porphyrin, pyrene and carbazole. Most of them focused on the improvement of the probes'

selectivity for G-quadruplex DNA. However, an ideal G-quadruplex probe should display several key features, including strong photostability and chemical stability, an intense emission enhancement in the presence of G-quadruplexes, excellent discrimination for G-quadruplex DNA over other forms of DNA, and low detection limit.

Ionic styryl dyes represent an important class of function dyes that have a number of favorable properties. They are fluorescent, have high photostability and synthetically easily available [27,28]. Some of them exhibited remarkably high affinities toward double-stranded DNA along with significant changes of their photo-physical properties [29,30]. Recently, our group has designed and synthesized several triphenylamine derivatives that exhibited good selectivity for G-quadruplex DNAs [31]. These derivatives contain an amine side chain, which is considered crucial for G-quadruplex DNA sensing. In order to enhance the selectivity and sensitivity toward G-quadruplex DNAs of the ionic styryl dyes, we attempted to assemble styrylquinolinium and amine side group in a fusion scaffold. Herein, we reported a new bis-amine-substituted styrylquinolinium dye (**BASQ**), which was synthesized by a simple and rapid process. The detailed interactions of **BASQ** with G-quadruplex DNAs were investigated.

2. Experimental methods

2.1. Oligonucleotides

All oligonucleotides (HPLC purified) were purchased from Sangon Biotechnology Co., Ltd. (Shanghai, China) and the sequences were listed in **Table S1**. Oligonucleotides were dissolved in 10 mM Tris-HCl buffer (containing 60 mM KCl, pH 7.4). Prior to use, all oligonucleotides were pre-treated by heating at 95 °C for 5 min, followed by gradual cooling to room temperature and kept at this temperature for 30 min. Binding experiments were performed in the same buffers as used to dissolve the oligonucleotides.

2.2. Synthesis and characterization

¹H NMR and ¹³C NMR spectra were measured on a 400 MHz spectrometer using TMS as internal standard in CDCl₃ or DMSO-*d*₆. Mass spectra (MS) were recorded on a Shimadzu LCMS-2010A instrument with an ESI detector. 4-Fluorobenzaldehyde, *N*-methyl piperazine and 4-hydroxy-2-methylquinoline were purchased from Beijing InnoChem Science & Technology Co., Ltd. All common solvents and chemical reagents were used as received without further purification. Stock solutions of **BASQ** (5 mM) were prepared in DMSO.

2.1.1. Synthesis and characterization of intermediate **1**

4-Fluorobenzaldehyde (400 mg, 3.22 mmol), *N*-methyl piperazine (322 mg, 3.22 mmol) and K₂CO₃ (469 mg, 3.40 mmol) were stirred in dry DMF at 130 °C under nitrogen atmosphere. After 12 h, the reaction was quenched by addition of water. The resulting mixture was extracted with EtOAc (3 × 50 mL), washed with brine, and dried over anhydrous Na₂SO₄. The resulting residue was purified by flash chromatography (PE/EtOAc 1:4). Yield 65%, white solid. ¹H NMR (400 MHz,

CDCl₃) δ 9.78 (s, 1H), 7.76 (d, $J = 8.8$ Hz, 2H), 6.92 (d, $J = 8.8$ Hz, 2H), 3.46-3.37 (m, 4H), 2.59-2.54 (m, 4H), 2.36 (s, 3H).

LC-MS: (positive mode, m/z) calculated 205.1431, found 205.1321 for [M+H]⁺.

2.1.2. Synthesis and characterization of **BASQ**

A solution of *intermediate 1* (320 mg, 1.59 mmol), 1,2-dimethyl-4-chloroquinolin-1-ium iodide (**3**, 507 mg, 1.59 mmol) and *N*-methyl piperazine (200 mg, 2.0 mmol) in anhydrous ethanol (30 mL) was refluxed for 24 h under nitrogen with stirring. After cooling to room temperature, the solvent was evaporated under reduced pressure. The residue was purified by column chromatography on silica gel eluting with CH₂Cl₂/CH₃OH (20:1, v/v) to afford **BASQ** (0.35 g, 38.7 %) as a red solid. ¹H NMR (400MHz, DMSO-*d*₆) δ : 8.24 (d, $J = 8.28$ Hz, 1H), 8.09 (d, $J = 7.84$ Hz, 1H), 7.99-7.90 (m, 2H), 7.78 (d, $J = 7.32$ Hz, 2H), 7.72 (t, $J = 6.6$ Hz, 1H), 7.47 (s, 1H), 7.43 (s, 1H), 7.01 (d, $J = 7.08$ Hz, 2H), 4.19 (s, 3H), 3.75 (br, 8H), 2.79-2.73 (m, 8H), 2.48 (s, 3H), 2.37 (s, 3H); ¹³C NMR (100 MHz, DMSO-*d*₆) δ : 158.86, 154.35, 151.67, 143.76, 140.54, 133.53, 130.35, 126.31, 126.14, 125.15, 119.62, 119.11, 115.02, 114.31, 104.86, 53.89, 53.42, 53.36, 51.12, 45.69, 45.04, 44.24; LC-MS: (positive mode, m/z) calculated 442.2965, found 442.2955 for [M-I]⁺.

2.3. Measurements and methodology

2.3.1. UV-vis spectral studies

The UV-vis spectra were recorded on an UV-2550 spectrophotometer using a 1 cm path length quartz cuvette at room temperature. For the titration experiments, small aliquots of a stock solution of the DNAs were added to the solution containing **BASQ** at a fixed concentration (8 μ M) in aqueous buffer (10 mM Tris-HCl, pH 7.4, 60 mM KCl). After each DNA addition, the solution was incubated for 1 min before absorption spectra recorded.

2.3.2. Fluorimetric titrations

Fluorescence spectra were measured on a Shimadzu RF-5301PCS spectrofluorophotometer in a 10 mm quartz cell at room temperature. The concentration of **BASQ** was fixed at 2 μ M and the titration process was similar to absorption spectra titration experiment. Both excitation and emission slits were set at 10 nm. The fluorescence measurement was obtained at an excitation wavelength of 470 nm. The data from the fluorimetric titrations were analyzed according to the independent-site model by nonlinear fitting to equation (1) [32], in which F_0 is the fluorescence intensity of **BSAQ** in the absence of G-quadruplex DNA, n is the putative number of **BASQ** molecules binding to a given DNA matrix, Q is the fluorescence enhancement upon saturation, $A = 1/[K_a C_{dye}]$ and $x = nC_{DNA}/C_{dye}$. The parameters Q and A were found by Levenberg-Marquardt fitting routine in Origin 8.5 software.

$$\frac{F}{F_0} = 1 + \frac{Q - 1}{2} \left[A + 1 + x - \sqrt{(A + 1 + x)^2 - 4x} \right] \quad (1)$$

2.3.3. FID assay

The experiment was carried out in 10 mM Tris-HCl buffer (containing 60 mM KCl, pH 7.4) by adding different concentrations of **BASQ** to the TO-bound Htg-21 solution. The concentrations of TO and Htg-21 were set at 0.5 and 0.1 μ M, respectively. **BSAQ** was added until no change was observed in the fluorescence intensity indicating the

binding saturation has been achieved. The fluorescence spectra were measured using excitation wavelength at 504 nm and the emission range was set between 515 and 700 nm.

2.3.4 Circular dichroism (CD)

CD spectra (230-400 nm) were performed on a JASCO-J815 circular dichroism spectrophotometer using a 10 mm path length quartz cuvette. The scanning speed of the instrument was set to 500 nm min⁻¹. The strand concentration of oligonucleotide Htg-21 used for measurement was 5 μM. The buffer condition is 10 mM Tris-HCl, pH 7.4 in the presence/absence of 60 mM KCl. Final analysis of the data was carried out using Origin 8.5.

3. Results and discussion

3.1 Synthesis of the bis-amine-substituted styrylquinolinium dye **BASQ**

The desired dye, **BASQ**, was synthesized following the procedure reported previously by our group [31]. As shown in **Scheme 1**, intermediate **1** was obtained by the reaction of *p*-fluorobenzaldehyde with *N*-methyl piperazine. This compound was followed by reaction with 1,2-dimethyl-4-chloroquinolin-1-ium iodide, *N*-methyl piperazine in one-pot to give the final dye **BASQ**. The structure of this new dye was characterized by ¹H NMR, ¹³C NMR and MS (see the Supplementary Information).

<*Scheme 1. Synthetic route for the synthesis of **BASQ**.*>

3.2 Fluorescence spectroscopic studies of **BASQ** upon interaction with nucleic acids

To investigate the interactions of **BASQ** with G-quadruplex DNAs, fluorescence titrations in 10 mM Tris-HCl buffer at pH 7.4 were first performed. The fluorescence emission band of **BASQ** (2 μM) at 514 nm is very weak at room temperature (**Fig.1**). Upon gradual addition of human telomeric G-quadruplex DNA Htg-21, an emission peak at approximately 587 nm appeared and was significantly enhanced and eventually reached to ~240 fold at the concentration as low as 0.68 μM. We speculated that the interaction between **BASQ** and Htg-21 may restrict the rotation of the methine-bridge of **BASQ**, as shown by the emission enhancement in a viscous medium (**Fig. S1**), therefore enhancing the radiative pathway relaxation and fluorescence emission [33]. This fluorescent turn-on properties were also observed when treated with other G-quadruplex DNAs (22AG, CM22, C-myc, G3T3, Hras and Ckit1) (**Fig.1B** and **Fig. S2**). The changes in fluorescence intensities could even be detected by the naked eye under UV light (**Fig. S3**). It is worth pointing out that the specific red emission of **BASQ** with G-quadruplex DNA is very attractive for cellular imaging experiments, as low photo-damage, and minimal fluorescence background can be achieved [34]. In contrast, much smaller changes were observed with single-stranded DNA (ss26), double-stranded DNA (ctDNA) and the protein BSA. These results suggest that **BASQ** exhibits a selectively fluorescence response toward G-quadruplex DNAs.

<Fig.1. (A) Fluorescence spectra of 2 μM **BASQ** titrated with Htg-21 in 10 mM Tris-HCl buffer, 60 mM KCl, pH 7.4; Arrow: concentrations of Htg-21 ranged from 0 to 0.68 μM . (B) Distribution of the values of fluorescence intensity at 587 nm for **BASQ** (2 μM) with all the tested samples (0.68 μM). Error bars represent the standard deviations of the results from three independent experiments.>

3.3 UV-vis spectroscopic studies of **BASQ** upon interaction with nucleic acids

The absorption properties of **BASQ** with nucleic acids were explored by UV-vis spectroscopic titrations. Electronic absorbance spectroscopy is one of the most useful tools to investigate the interactions of dyes with DNA. As shown in **Fig. 2A**, upon addition of Htg-21, the intensity of 377 nm gradually decreased, and a large redshift of the maximum was observed with an obvious isosbestic point at 433 nm, which finally led to a new peak at about 456 nm. Other tested G-quadruplex DNAs could also clearly enhance the absorbance of **BASQ** at 456 nm (**Fig. S4**). It has been reported that intercalative mode of binding between compound and DNA usually results in hypochromism and red shift due to the strong stacking interactions [35]. The large red shift and hypochromism between **BASQ** and G-quadruplexes parallels intercalative binding mode. In general, quinolinium moiety may interact with G-quartet plane by π - π stacking. The effects of duplex and single-stranded DNAs on the absorption bands of **BASQ** were much weaker than the G-quadruplex DNAs, which only caused a hypochromic effect at 433 nm. Thus, the value of $A_{456\text{ nm}}/A_{377\text{ nm}}$ could be used as a criterion to discriminate between G-quadruplexes and other DNA forms. At the concentration of 2.4 μM DNA, The values of $A_{456\text{ nm}}/A_{377\text{ nm}}$ of all tested G-quadruplexes were greater than 1.0. In contrast, the values of other DNAs were less than 0.75 (**Fig. 2B**). Accordingly, the changes in absorption spectra were in good agreement with that of fluorescence titration experiments. The above results indicate that **BASQ** could also be used as a colorimetric probe to distinguish G-quadruplexes from other DNA forms.

<Fig.2. (A) Absorption spectra of 8 μM **BASQ** titrated with Htg-21 in 10 mM Tris-HCl buffer, pH 7.4, 60 mM KCl; Arrows: concentrations of Htg-21 ranged from 0 to 2 μM . (B) Plots of $A_{456\text{ nm}}/A_{377\text{ nm}}$ of 8 μM **BASQ** against the DNA concentrations.>

3.4. The detection limits of **BASQ** with G-quadruplex DNAs

For an ideal G-quadruplex DNA probe, the selectivity and sensitivity are both important criteria. Therefore, we measured the detection limits (LODs) of **BASQ** toward DNA G-quadruplexes by means of spectrofluorimetric titrations. The LOD values were calculated according to the equation $3\sigma/k$ [36]. The σ value represents the standard deviation for multiple measurements of blank solution. The k value is the slope derived from the linear range of the **BASQ** fluorescence titration curve with different G-quadruplex DNAs. The linear ranges of the fluorescence titration curves for **BASQ** with most of G-quadruplex DNAs ranged from 0-400 nM. Thus, the k values were obtained by fitting these curves and the corresponding values of the LODs were shown in **Table 1** and **Fig. S5**. Clearly, the LODs of **BASQ** for different G-quadruplex DNAs in

ACCEPTED MANUSCRIPT

solution were below 1 nM, which meant it was able to detect G-quadruplex DNAs in the nanomolar range. It is also noteworthy that the LOD values of **BASQ** are significantly improved in comparison with mono-amine-substituted quinolinium dye reported previously [31], which has a detection limit of 158 nM. Accordingly, the improving detection limits of **BASQ** for G-quadruplex DNA revealed the importance of the amine chain. The data underline that **BASQ** shows high sensitivity toward G-quadruplex DNAs.

<Table 1 The detection limits and linear ranges of **BASQ** (2 μ M) for different G-quadruplex DNAs in solution.>

3.5. Binding properties of **BASQ** with G-quadruplex DNAs

In an effort to understand the details of binding process, we evaluated the binding stoichiometries and intrinsic constants (K_a) between **BASQ** and individual G-quadruplexes. The fluorescence titration curves were further fitted to an independent-site model (Experimental methods). The results are summarized in **Table 2**. Analyses of the relationship between the fluorescence intensity of **BASQ** and the concentrations of DNA G-quadruplexes afforded binding constants in the range from 0.10-3.36 $\times 10^6$ M⁻¹. However, the binding affinities and fluorescence enhancements are not directly correlated, due to the different microenvironments in the binding sites, which avoid the nonradiative relaxation process to different extents. The results were further confirmed by Job plot experiments (**Fig. S6**). To gain further insight into the binding mode between **BASQ** and G-quadruplex, the dye affinity for Htg-21 was tested by an indirect FID (fluorescence intercalator displacement) approach [37]. This assay measures the decrease in fluorescence intensity upon the displacement of thiazole-orange (TO) from the G-quadruplex-TO complex by the dye. TO is highly fluorescent upon interaction with G-quadruplex DNA mainly by a π - π stacking mode whereas totally quenched when free in solution. Efficiency TO displacement would thus be an indication of a same binding mode of our dye. As shown in Fig S7, **BASQ** could partially displace (41%) TO from Htg-21, indicating the fact that quinolinium moiety of **BASQ** can only undergo partial stacking interactions with G-quadruplex DNA.

<Table 2. Binding stoichiometries and intrinsic binding constants (K_a) of **BASQ** in the presence of different G-quadruplex DNAs.>

3.6. Effect of cationic species of Htg-21 on the interactions with **BASQ**

Since the G-rich sequence is prone to fold into G-quadruplex structure in the presence of metal ions. And cationic ion plays an important role in determining the secondary structures [5,6]. To explore this, the fluorescence behaviors of **BASQ** with Htg-21 in the different concentrations of K⁺ ion were investigated. The finding showed that fluorescence intensities of **BASQ** strongly depended on the concentrations of K⁺ ion, with maximal value occurring near 5 mM. Above this

concentration, however, the maximum fluorescence intensity was found to show a regular decrease, perhaps because the high concentration of K^+ disrupted the docking between the Htg-21 and **BASQ**. Based on the G-quadruplex ligands reported previously, we have known that the positively charged or protonable amine side group would enhance electrostatic interaction strength with the negatively charged DNA phosphate backbone. The strong dependence of the fluorescence intensities on the ionic strength of the buffer indicates that the electrostatic interactions play an important role in the binding process.

<Fig.3. (A) Fluorescence intensities of **BASQ** ($2 \mu M$) at 587 nm with different amounts of Htg-21 in the various K^+ buffers (1-100 mM). (B) Fluorescence intensities of **BASQ** ($2 \mu M$) at 587 nm with Htg-21 ($0.32 \mu M$) in the 1-100 mM K^+ buffers.>

3.7. CD studies

To investigate whether **BASQ** has the G-quadruplex induced ability with Htg-21 which can not spontaneously fold into G-quadruplex in the absence of metal ion K^+ , the effects of **BASQ** on the conformation of G-quadruplex Htg-21 in the absence and presence of K^+ ion were studied by using circular dichroism (CD), which is an extremely useful technique to study nucleic acids conformation. The typical CD spectrum of Htg-21 is a hybrid-type of quadruplex DNA containing parallel and anti-parallel structure in the presence of K^+ ion, with a large positive band at about 293 nm, a shoulder around 272 nm, a small positive band at 251 nm, and a minor negative band near 234 nm [6,38,39]. Upon gradual addition of **BASQ** to this solution, a maximum band at 292 nm increased and the shoulder at 272 nm decreased and merged into the band at 292 nm. Meanwhile, the small positive band at 251 nm decreased. These changes indicated that the dye **BASQ** did not cause significant conformation transition of Htg-21 G-quadruplex structure. However, the enhancement of the positive peak may be attributed to the stabilization of G-quadruplex structure by this dye. In order to explore whether **BASQ** can induce the formation of G-quadruplex structure or not in the absence of salt, the CD experiment was carried out in the K^+ -free buffer. In this case, the Htg-21 alone displayed a characteristic CD band at 255 nm and 297 nm, conforming its unfolded state (Fig. 4B). As the concentration of **BASQ** increased, there were still two characteristic positive CD band at 255 nm and 297 nm, confirming its unfolded state, indicating that **BASQ** can not induce the structure exchange from unfolded state to quadruplex state.

<Fig. 4. CD titrations spectra of **BASQ** for Htg-21 ($4 \mu M$) in 10 mM Tris-HCl buffer (pH 7.4) in the presence (A) and absence (B) of 60 mM KCl. The concentration of **BASQ** is from 0 to 8 μM . Arrows indicate the change direction of peaks.>

4. Conclusions

In conclusion, a bis-amine-substituted styryl dye, **BASQ**, has been designed and synthesized as a G-quadruplex DNA

targeting probe. **BASQ** was found to express large red shifts of its absorption spectra and significant fluorescence enhancements upon binding with G-quadruplex DNAs, while showed insignificant changes upon interactions with non-quadruplex structures. In further studies, **BASQ** exhibited highly sensitive fluorescence detection of G-quadruplex DNAs with the LOD values below 1 nM in solution. The CD spectra titrations results revealed that **BASQ** could not convert G-rich sequence into G-quadruplex structure. All these remarkable properties of **BASQ** suggested it should have promising applications in the field of G-quadruplex DNA research, and provide useful information for future studies.

Authors Informations

* Corresponding author.

** Corresponding author.

E-mail addresses: wmq3415@163.com (M.-Q. Wang), chenqy@ujs.edu.cn

Acknowledgements

This work was financially supported by the China Postdoctoral Foundation (Grant No. 2017M611704), Senior Talent Cultivation Program of Jiangsu University (Nos. 15JDG068), National Natural Science Foundation of China (21571085).

Appendix A. Supplementary date

Supplementary date related to this article can be found at XXXXXX.

References

- [1] Wu L, Qu X. Cancer biomarker detection: recent achievements and challenges. *Chem Soc Rev* 2015; 44(10):2963-97.
- [2] Rhodes D, Lipps HJ. G-quadruplexes and their regulatory roles in biology. *Nucleic Acids Res* 2015; 43(18):8627-37.
- [3] Huppert JL. Structure, location and interactions of G-quadruplexes. *FEBS J* 2010; 277:3452-8.
- [4] Cimino-Reale G, Zaffaroni N, Folini M. Emerging Role of G-quadruplex DNA as Target in Anticancer Therapy. *Curr Pharm Design* 2016; 22(44):6612-24.
- [5] Gellert M, Lipsett MN, Davies DR. Helix formation by guanylic acid. *Proc Natl Acad Sci USA* 1962; 48:2013-2018.
- [6] Burge S, Parkinson GN, Hazel P, Todd AK, Neidle S. Quadruplex DNA: Sequence, topology and structure. *Nucleic Acids Res* 2006; 34:5402-15.
- [7] Stegle O, Payet L, Mergny JL, MacKay DC, Huppert JL. Predicting and understanding the stability of G-quadruplexes. *Bioinformatics* 2009; 25(12):374-82.
- [8] Huppert JL, Balasubramanian S. Prevalence of quadruplexes in the human genome. *Nucleic Acids Res* 2005; 33(9): 2908-16.
- [9] Bidzinska J, Cimino-Reale G, Zaffaroni N, Folini M. G-Quadruplex Structures in the Human Genome as Novel Therapeutic Targets. *Molecules* 2013; 18(10):12368-395.
- [10] Lipps HJ, Rhodes D. G-quadruplex structures: in vivo evidence and function. *Trends cell biol* 2009; 19(8): 414-422.
- [11] Bochman ML, Paeschke K, Zakian VA. DNA secondary structures: stability and function of G-quadruplex structures. *Nat Rev Genet* 2012; 13:770-80.
- [12] Dolinnaya NG, Ogloblina AM, Yakubovskaya MG. Structure, properties, and biological relevance of the DNA and RNA G-quadruplexes: Overview 50 years after their discovery. *Biochemistry-moscow* 2016; 81:1602-49.
- [13] Biffi G, Tannahill D, McCafferty J, Balasubramanian S. Quantitative visualization of DNA G-quadruplex structures in human cells. *Nat Chem* 2013; 5: 182-86.
- [14] Ma D-L, Zhang Z, Wang M, Lu L, Zhong H-J, Leung C-H. Recent Developments in G-Quadruplex Probes. *Chem Biol* 2015; 22:812-28.
- [15] Ma DL, Wang M, Lin S, Han QB, Leung CH. Recent Development of G-Quadruplex Probes for Cellular Imaging. *Curr Top Med Chem* 2015;15(19):1957-63.
- [16] Vummidi BR, Alzeer J, Luedtke NW, Fluorescent Probes for G-Quadruplex Structures. *Chembiochem* 2013; 14(5):540-58.

- [17] Chen X, Wang J, Jiang GM, Zu GY, Liu M, Zhou L. et al. The development of a light-up red-emitting fluorescent probe based on a G-quadruplex specific cyanine dye. *RSC Adv* 2016; 6(74):70117-23.
- [18] Hu MH, Guo RJ, Chen SB, Huang ZS, Tan JH. Development of an engineered carbazole/thiazole orange conjugating probe for G-quadruplexes. *Dyes Pigments* 2017; 137:191-199.
- [19] Yang P, Cian AD, Teulade-Fichou M-P, Mergny J-L, Monchaud D. Engineering Bisquinolinium/Thiazole Orange Conjugates for Fluorescent Sensing of G-Quadruplex DNA. *Angew Chem Int Ed* 2009; 48:2188-91.
- [20] Wu SR, Wang LL, Zhang N, Liu Y, Zheng W, Chang A. et al. A Bis(methylpiperazinylstyryl)phenanthroline as a Fluorescent Ligand for G-Quadruplexes. *Chem-Eur J* 2016; 22(17):6037-47.
- [21] Wu F, Liu CX, Chen YQ, Yang SX, Xu JH, Huang R. et al. Visualization of G-quadruplexes in gel and in live cells by a near-infrared fluorescent probe. *Sensor Actuat B-Chem* 2016; 236:268-75.
- [22] Lu Y-J, Deng Q, Hou J-Q, Hu D-P, Wang Z-Y, Zhang K. et al. Molecular Engineering of Thiazole Orange Dye: Change of Fluorescent Signaling from Universal to Specific upon Binding with Nucleic Acids in Bioassay. *ACS Chem Biol* 2016; 11:1019-29.
- [23] Seo YJ, Lee IJ, Yi JW, Kim BH. Probing the stable G-quadruplex transition using quencher-free end-stacking ethynyl pyrene-adenosine. *Chem Commun* 2007; 27:2817-9.
- [24] Kim HN, Lee E-H, Xu Z, Kim H-E, Lee H-S, Lee J-H. et al. A pyrene-imidazolium derivative that selectively Recognizes G-Quadruplex DNA. *Biomaterials* 2012; 33(7):2282-8.
- [25] Chen S-B, Hu M-H, Liu G-C, Wang J, Ou T-M, Gu L-Q, et al. Visualization of NRAS RNA G-Quadruplex Structures in Cells with an Engineered Fluorogenic Hybridization Probe. *J. Am. Chem. Soc.* 2016; 138(33): 10382–5.
- [26] Laguerre A, Hukezalie K, Winckler P, Katranji F, Chanteloup G, Pirrotta M. et al. Visualization of RNA-Quadruplexes in Live Cells. *J. Am. Chem. Soc.* 2015; 137(26): 8521–5.
- [27] Deligeorgiev T, Vasilev A, Kaloyanova S, Vauero JJ. Styryl dyes—synthesis and applications during the last 15 years. *Color Technol* 2010; 126:55- 80.
- [28] Xie X, Choi B, Largy E, Guillot R, Granzhan A, Teulade-Fichou M-P. Asymmetric Distyrylpyridinium Dyes as Red-Emitting Fluorescent Probes for Quadruplex DNA. *Chem Eur J* 2013; 19:1214-26.
- [29] Feng S, Kim YK, Yang S, Chang Y-T. Discovery of a green DNA probe for live-cell imaging. *Chem Commun* 2010; 46:436-8.
- [30] Macoas E, Marcelo G, Pinto S, CaÇeque T, Cuadro AM, Vaquero JJ. et al. A V-shaped cationic dye for nonlinear optical bioimaging. *Chem Commun* 2011; 47:7374-6.
- [31] Wang M-Q, Zhu W-X, Song Z-Z, Li S, Zhang Y-Z. A triphenylamine-based colorimetric and fluorescent probe with donor–bridge–acceptor structure for detection of G-quadruplex DNA. *Bioorg Med Chem Lett* 2015; 25:5672-6.
- [32] Stootman FH, Fisher DM, Rodger A, Aldrich-Wright JR. Improved curve fitting procedures to determine equilibrium binding constants. *Analyst* 2006; 131:1145-51.
- [33] Yan JW, Chen SB, Liu HY, Ye WJ, Ou TM, Tan JH, et al. Development of a new colorimetric and red-emitting fluorescent dual probe for G-quadruplex nucleic acids. *Chem Commun* 2014; 50:6927-30.
- [34] Yuan L, Lin W, Zheng K, He L, Huang W. Far-red to near infrared analyte-responsive fluorescent probes based on organic fluorophore platforms for fluorescence imaging. *Chem Soc Rev* 2013; 42:622-61.
- [35] Tarushi A, Kljun J, Turel I, Pantazaki AA, Psomas G, Kessissoglou DP. Zinc(II) complexes with the quinolone antibacterial drug flumequine: structure, DNA- and albumin-binding. *New J Chem* 2013; 37:342-55.
- [36] Shortreed M, Kopelman R, Kuhn M, Hoyland B. Fluorescent fiber-optic calcium sensor for physiological measurements. *Anal Chem* 1996; 68(8):1414-8.
- [37] Nguyen BT, Anslyn EV. Indicator–displacement assays. *Coord Chem Rev* 2006, 250:3118-27.
- [38] Shirude, P. S.; Gillies, E. R.; Ladame, S.; Godde, F.; Shin-ya, K.; Huc, I.; Balasubramanian, S. *J. Am. Chem. Soc.* 2007, 129, 11890-11891;

Scheme 1 Synthetic route for the synthesis of **BASQ**.

Table 1 The detection limits and linear ranges of **BASQ** (2 μM) for different G-quadruplex DNAs in solution.

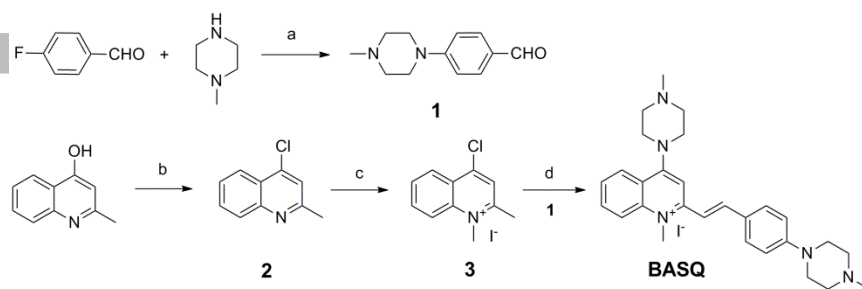
Table 2 Binding stoichiometries and intrinsic binding constants (K_a) of **BASQ** in the presence of different G-quadruplex DNAs.

Fig. 1. (A) Fluorescence spectra of 2 μM **BASQ** titrated with Htg-21 in 10 mM Tris-HCl buffer, 60 mM KCl, pH 7.4; Arrow: concentrations of Htg-21 ranged from 0 to 0.68 μM . (B) Distribution of the values of fluorescence intensity at 587 nm for **BASQ** (2 μM) with all the tested samples (0.68 μM). Error bars represent the standard deviations of the results from three independent experiments.

Fig. 2. (A) Absorption spectra of 8 μM **BASQ** titrated with Htg-21 in 10 mM Tris-HCl buffer, pH 7.4, 60 mM KCl; Arrows: concentrations of Htg-21 ranged from 0 to 2 μM . (B) Plots of $A_{456\text{ nm}}/A_{377\text{ nm}}$ of 8 μM **BASQ** against the DNA concentrations.

Fig. 3. (A) Fluorescence intensities of **BASQ** (2 μM) at 587 nm with different amounts of Htg-21 in the various K^+ buffers (1-100 mM). (B) Fluorescence intensities of **BASQ** (2 μM) at 587 nm with Htg-21 (0.32 μM) in the 1-100 mM K^+ buffers.

Fig. 4. CD titrations spectra of **BASQ** for Htg-21 (4 μM) in 10 mM Tris-HCl buffer (pH 7.4) in the presence (A) and absence (B) of 60 mM KCl. The concentration of **BASQ** is from 0 to 8 μM . Arrows indicate the change direction of peaks.



Reagents and conditions: (a) potassium carbonate, 100 °C, 12 h; (b) phosphorus oxychloride, 120 °C, 5 h; (c) iodomethane, sulfolane, 80 °C 24 h; (d) *N*-methyl piperazine, 1, ethanol, 80 °C, 12 h.

Scheme 1

DNA sample	LOD (nM)	Linear range (nM)
Htg-21	0.84	0-400
22AG	0.63	0-240
C-myc	0.36	0-320
CM22	0.64	0-400
Ckit1	0.72	0-400
G3T3	0.63	0-320
Hras	0.85	0-320

Table 1

DNA sample	Stoichiometry (BASQ:DNA)	K_a (10^6 M^{-1})
Htg-21	2:1	0.91 ± 0.07
22AG	1:1	0.62 ± 0.05
C-myc	4:1	0.22 ± 0.02
CM22	2:1	0.10 ± 0.01
Ckit1	1:2	0.56 ± 0.04
G3T3	4:1	3.36 ± 0.12
Hras	4:1	3.01 ± 0.11

Table 2

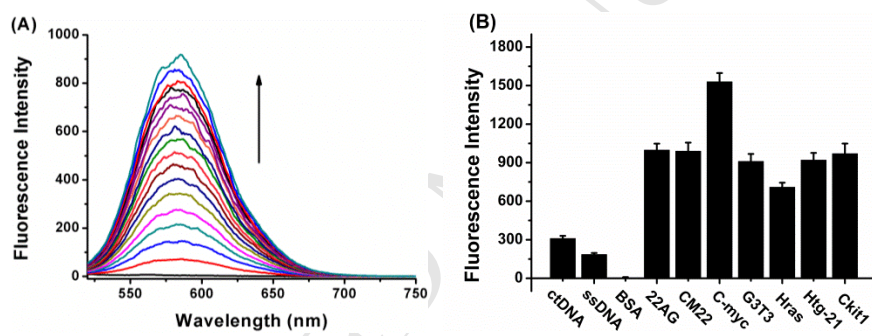


Fig. 1

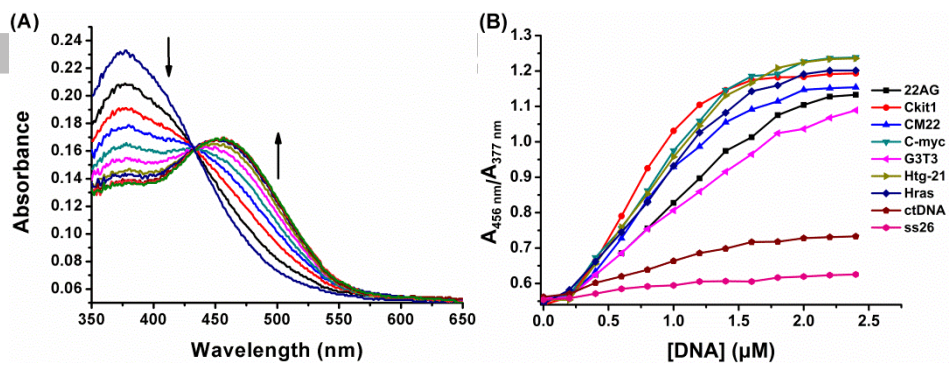


Fig. 2

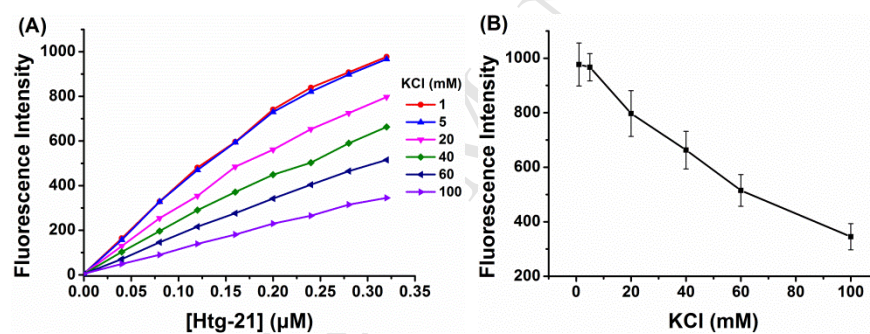


Fig. 3

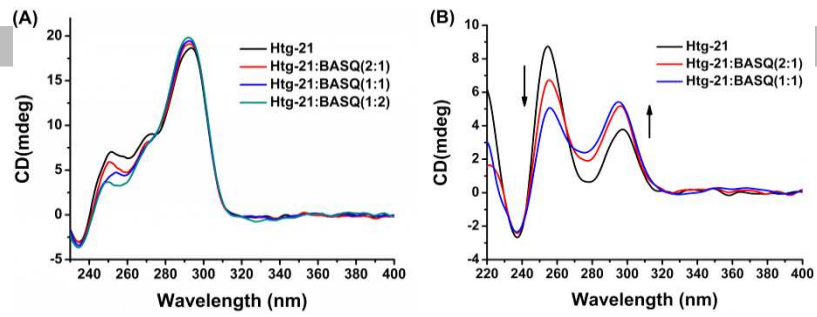


Fig. 4

ACCEPTED MANUSCRIPT

Highlights:

A bis-amine-substituted styrylquinolinium dye (**BSAQ**) was designed and synthesized.

BSAQ could be used as a colorimetric and red-emitting fluorescent probe for G-quadruplex DNAs.

The limits of detection of **BSAQ** with various G-quadruplex DNAs were found to below 1 nM.

The binding properties were demonstrated.

ACCEPTED MANUSCRIPT